Enhanced piecewise least squares approach for diagnosis of ill-conditioned multistation assembly with compliant parts

D Ceglarek[1,2] and **PKS Prakash**[1,2,3]*
[1]International Digital Laboratory, WMG, University of Warwick, Coventry, UK
[2]Department of Industrial and Systems Engineering, University of Wisconsin-Madison, Madison, Wisconsin, USA
[3]The Irish Centre for Manufacturing Research, NUI, Maynooth, County Kildare, Republic of Ireland

The manuscript was received on 3 May 2011 and was accepted after revision for publication on 24 August 2011.

DOI: 10.1177/0954405411423458

Abstract: Assembly process-induced dimensional variation has a significant impact on product quality and functionality. The complexity of modern products coupled with part compliance/flexibility frequently results in ill-conditioned assembly systems further adding to the challenges of process control and fault failure diagnosis. This paper proposes an enhanced piecewise least squares (EPLS)-based approach for dimensional fault failure diagnosis of ill-conditioned multistation assembly systems. In this approach, predetermined fault patterns derived from an inverse stiffness matrix of assembly structures and fault patterns obtained from product measurement data are used to detect and isolate dimensional failures caused by fixturing error(s). The EPLS-based diagnostic methodology searches for a set of components called *latent vectors* with the search constrained by assembly response function, the stream of variation analysis (SOVA) model of an assembly system, which performs decomposition of response based on the end-of-line measurements. The verification of the proposed methodology is conducted based on a beam-based model of a multistation assembly process with compliant parts and includes diagnosis of both single and multiple fault scenarios.

Keywords: dimensional variation, assembly, process control, fault diagnosis

1 INTRODUCTION

Manufacturing firms are perpetually aiming to reduce their internal and external lead time to launch new products in order to respond to changing customer needs. One of the major challenges towards reducing the internal lead time during a new product development is the long production ramp-up time. To respond to this prolonged lead time, firms need to assess and respond to the necessary product and process design changes as well as process adjustments that occur during the ramp-up and production phase. Two-thirds of all process design changes during the launch of a new assembly process in automotive and aerospace industries are caused by dimensional failures/variation [**1**, **2**]. Hence, dimensional quality control is a major challenge within manufacturing industries. Additionally, 70–75 per cent of root causes of product dimensional variations are due to fixture-related problems. In the automotive body assembly process of sport utility vehicles, about 63 per cent of fixtures have a 3–2–1 layout as used for rigid parts and about 37 per cent of fixtures have a non-3–2–1 layout, specifically *N*–2–1 fixture layouts as used predominantly for compliant sheet metal parts. However, currently there is only limited development in the diagnosis of dimensional variation root causes for assembly processes with compliant parts.

Dimensional quality is a measure of conformance between the actual geometry of manufactured

*Corresponding author: The Irish Centre for Manufacturing Research, NUI, Maynooth, County Kildare, Republic of Ireland. email: prakash@nuim.ie

products and their designed geometry. Thus, the dimensional integrity of each subassembly might exert a tremendous impact on the quality of the final product. Traditional methods for quality improvement are primarily based on statistical analysis of measurement data obtained from production, which focuses on process inspection and process change detection rather than root cause determination. However, these methods are inadequate for the purposes of fault determination in complex multistation assembly systems involving high-volume production such as automotive or aerospace body assembly. Therefore, proper fixture design is crucial to workpiece quality assurance in manufacturing. However, even the best-designed fixture with proper layout of locating pins and blocks is bound to wear out, bend, or break over a period of time. The worn fixture can lead to severe deterioration in the ability of the fixture to locate accurately the part causing quality problem(s) in the final product.

The main causes of dimensional variations in compliant assembly can be classified into four categories: (i) part variation due to errors in fabrication processes; (ii) part positioning and clamping error in assembly fixture; (iii) part/subassembly variation due to the joining process [**2**, **3**]; and (iv) part/subassembly springback due to part release in the assembly station.

Currently, the state-of-the-art research focuses on diagnosing faulty 3–2–1 fixtures that can cause dimensional variations in the final product during the assembly process. The current methods are based on the development of predetermined fault variation patterns obtained based on computer aided design (CAD) information, fault variation patterns obtained from measurement data, and fault pattern recognition/mapping procedures.

This paper develops a methodology to address the following key points: (i) diagnosis of dimensional failures; (ii) modelling of a multistation assembly process with compliant parts; and (iii) ill-conditioned design of the assembly system, especially ill-conditioned systems described by negative colinearity. The ill-conditioned system refers to situations where variations in key control characteristics lead to variation patterns that are near parallel, thus resulting in widely discrepant results for relations between key control characteristics and key product characteristics. The proposed methodology will provide industries with the capability to respond quickly in the case of fault failure, thereby helping them to: (i) reduce ramp-up time by eliminating preproduction faults; (ii) improve product quality; (iii) enhance system productivity; and (iv) process maintenance.

Table 1 summarizes the current research done in the area of fixture layout design, variation propagation modelling, and diagnosis of fault variation patterns caused by fixture failure. From Table 1 it can be seen that most of the work in fixture diagnostics is carried out for rigid assembly systems and research on compliant assembly diagnostics is limited to single fault scenarios that occur in single assembly station or orthogonal multistation assembly systems.

Specifically, the diagnostic approach involving single faults in a single assembly fixture was proposed by Ceglarek and Shi [**12**]. This work was extended to diagnosis of a multistation assembly system first by Ceglarek *et al.* [**9**] and Shiu *et al.* [**19**] using heuristics models and then by Jin and Shi [**15**] and Ding *et al.*

Table 1 Comparison of fixture diagnostic methodologies

Assembly domain		Scope of research	Modelling of fixture layout	Modelling of part variation patterns caused by fixtures	Diagnostics of part variation pattern caused by fixtures
Rigid parts	3–2–1	Single station	Asada and By [**4**] Ferreira *et al.* [**5**] Chou *et al.* [**6**]	Ceglarek *et al.* [**9**] Ceglarek and Shi [**10**]	Ceglarek *et al.* [**9**]
			Wang and Pelinescu [**7**] Choubey *et al.* [**8**]	Zhou *et al.* [**11**]	Ceglarek and Shi [**12**]
		Multistation	Rong *et al.* [**13**]	Jin and Shi [**15**] Ding *et al.* [**16**]	Shiu *et al.* [**19**] Chang and Gossard [**20**]
			Rong and Bai [**14**]	Huang and Shi [**17**, **18**]	Apley and Shi [**21**]
Compliant parts	*N*–2–1	Single station	Menassa and DeVries (4–2–1) [**22**] Cai *et al.* [**23**] Sayeed and De Meter [**24**]	Liu and Hu [**25**]	Camelio and Hu (4–2–1) [**26**] Liu and Hu [**27**]
		Multistation (orthogonal design)	Xiong *et al.* [**28**]	Shiu *et al.* [**2**, **3**] Camelio *et al.* [**29**–**32**]	Rong *et al.* [**33**]
		Multistation (ill-conditioned design)	–	–	Rong *et al.* [**34**]* Method developed in this paper

*The method proposed by Rong *et al.* (2001) provides a poor solution for ill-conditioned systems with negative collinearity (Peres and DaCamara, 2004) [**35**].

[36] using a state-space modelling technique. Wang and Nagarkar [37], Khan and Ceglarek [38], Khan *et al.* [39], and Ding *et al.* [40] studied approaches of improving fault diagnosis based on the optimization of locators and sensor placement for assembly systems with rigid parts [41].

Extensive literature exists in the area of modelling and diagnosis of assembly processes with compliant parts. The modelling of a sheet metal assembly, which considers compliant variation sources such as part variation, fixture variations, and welding gun variations is studied by Camelio *et al.* [29]. Shiu *et al.* [2] proposed a beam-based model for dimensional control of compliant assemblies. Rong *et al.* [33] developed a diagnostic approach based on the beam-based model of an automotive body and principal component analysis (PCA) to isolate a single fault in compliant assemblies. Chang and Gossard [20] studied the impact of compliant non-ideal parts and locators using a CAD model. Recently, Apley and Shi [21] have extended the diagnosis of fixture failures in automotive body (body-in-white, BIW) assembly processes to detect multiple faults using the least squares (LS) approach for parts supported by the 3–2–1 fixturing scheme. The LS approach proposed by Apley and Shi [21] is a common technique for parameter estimation and for multiple fault diagnosis; however, this approach is insufficient in the case of an ill-conditioned system. Researchers have demonstrated that when a system is ill-conditioned, the parameter estimations based on the LS approach tend to be inflated, and there is a possibility that some of the estimations may be imprecise [42–44]. As a result, the LS solutions will lose the optimal properties of having a minimal 2-norm. In order to overcome problems related to an ill-conditioned system, Rong *et al.* [34] have proposed unrotated singular value decomposition (SVD) and matrix partitioning techniques. Unrotated SVD primarily determines empirical orthogonal functions (EOFs) based on the shape of the measurement data without taking into consideration the correlation between CAD design and production data. Thus, the SVD and matrix partitioning techniques allow identification of the linear combinations of faults that generate similar fault signatures, though it is generally inadequate for isolating individual modes of variation for cases with negative colinearity [35]. The cases of faults with negative colinearity are quite common in compliant assemblies in multistation assembly systems with *N*–2–1 fixtures (Fig. 1).

In this paper, a new enhanced piecewise least squares (EPLS) approach is developed to address the aforementioned problems related to SVD and matrix partitioning techniques. The proposed EPLS approach allows multiple faults predictive models to be constructed for ill-defined multistation assembly systems with large numbers of highly collinear factors. The EPLS approach works on the principle of extracting those latent vectors that account for meaningful variation by constraining each latent vector by an assembly response function model called the stream of variation analysis (SOVA), which models dimensional variation (six-sigma) propagation in an assembly system.

The remainder of the paper is organized as follows. Section 2 presents the variation propagation model for an *N*–2–1 fixture layout. Section 3 details the proposed methodology for fault isolation using the proposed enhanced piecewise least squares (EPLS) approach. To illustrate and validate the proposed methodology, simulation results using single- and two-fault case scenarios for a beam-based model of a multistation assembly process with compliant parts are presented in section 4. Finally, conclusions are summarized in section 5.

2 VARIATION PROPAGATION MODEL FOR AN N–2–1 FIXTURE LAYOUT

This section summarizes the variation propagation model for a multistation assembly system with

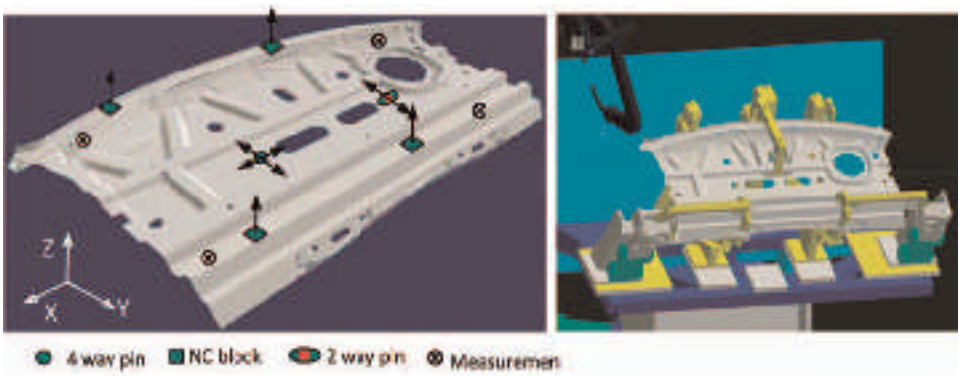

Fig. 1 Illustration of an *N*–2–1 fixturing scheme, where $N = 4$

compliant parts, known as the SOVA model. The SOVA model, based on a single station model [**12**], was developed by Jin and Shi [**15**], Ding *et al.* [**16**], and Ceglarek *et al.* [**45**] for rigid parts and then Huang *et al.* [**46**, **47**] extended it for rigid three-dimensional models for single- as well as multistation assembly processes. Camelio *et al.* [**29**] extended SOVA for a multistation process with compliant parts. Automotive body or aerospace fuselage assembly processes are examples of processes conducted in a hierarchical multistation architecture with fixtures locating each part and subassembly placed in each station or process stage. Both automotive and aerospace assembly processes use *N*–2–1 fixture layouts, where $N = 3$ is for rigid parts and $N > 3$ is for compliant sheet metal parts. In general, the variation propagation error caused by *N*–2–1 assembly fixtures can be decomposed into variation errors related to the main 6 degrees of freedom (DOFs) of a part or subassembly constrained by the basic 3–2–1 locating layout of the *N*–2–1 fixture and the other $(N - 3)$ DOFs constrained by the remaining $(N - 3)$ locators of the *N*–2–1 fixture.

Figure 2 represents the SOVA model for a multistage assembly process with K the number of stations, k indicating the station index, $X(k) \in R^{m\times 1}$ represents a state vector consisting of m number of product structural faults caused by the errors related to key control characteristics (KCCs), which occur due to part-to-part interference at station k; $\mathbf{U}(k) \in R^{q\times 1}$ represents the process fault due to fixturing error or part fabrication error, and q is a number of process variation sources at the kth station. The quality of the product can be expressed by the measurement matrix $\mathbf{Y}(k) \in R^{n\times 1}$ representing measurements taken at key product characteristics (KPCs), where n represents the number of measurements taken at station k; $\mathbf{w}(k) \in R^{m\times 1}$ and $\xi(k) \in R^{n\times 1}$ represent process and measurement errors observed at station k respectively. The measurement noise and process noise are considered to be independent of each other. Further, measurement noise is considered to have zero mean and σ_c^2 variance at all stations.

The quality of subassemblies at station k represented as $\mathbf{X}(k)$ is determined by the process fault $\mathbf{U}(k)$, quality of incoming parts/subassemblies $\mathbf{X}(k-1)$ and process random error $\mathbf{w}(k)$ at station k. Thus, the variation propagation model for a multistage assembly system with compliant parts can be represented as a linear state-space model as

$$\mathbf{X}(k) = \mathbf{A}(k-1)\mathbf{X}(k-1) + \mathbf{B}(k)\mathbf{U}(k) + \mathbf{w}(k) \quad (1)$$

$$\mathbf{Y}(k) = \Gamma(k)\mathbf{X}(k) + \xi(k) \quad (2)$$

where $\mathbf{A}(k-1)$ is the state matrix and $\mathbf{B}(k)$ is the input matrix. The state matrix $\mathbf{A}(k)$ is a function of parts/subassemblies reorientation effect between the station caused by the changing locating layout, **M**, part deformation before welding operation, **P**, and spring back effect, **R,** and can be represented as

$$\mathbf{A}(k) = f(\mathbf{M}(k), \mathbf{P}(k), \mathbf{R}(k)) \quad (3)$$

where matrix **M** is estimated based on the position of the locating fixtures and matrices **P** and **R** are generated using a finite element simulation of each stage. $\mathbf{A}(k-1)\mathbf{X}(k-1)$ represents the transformation of quality information from station $k-1$ to station k. $\mathbf{B}(k)\mathbf{U}(k)$ represents the process faults that occur due to fixturing error or part fabrication error at station k. $\Gamma(k)$ is the observation matrix, which represents the distribution of measurement stations and the layout of measurement points in each measurement station. For a measurement station located after any assembly station k, $\Gamma(k) \neq 0$ for $k = 1, \ldots, K$. The case $\Gamma(k) \neq 0$ only for $k = K$ produces a case with an end-of-line measurement station. A layout of measurement points in station k is represented by non-zero elements of matrix $\Gamma(k)$. $\mathbf{A}(k-1)$, $\mathbf{B}(k)$, and $\Gamma(k)$ are constant matrices for a given product and process design and can be determined based on the CAD/CAM model.

Based on the SOVA model, a diagnostics of a multistation assembly system can be formulated as

$$\mathbf{Y} = \mathbf{D}\mathbf{X} + \xi \quad (4)$$

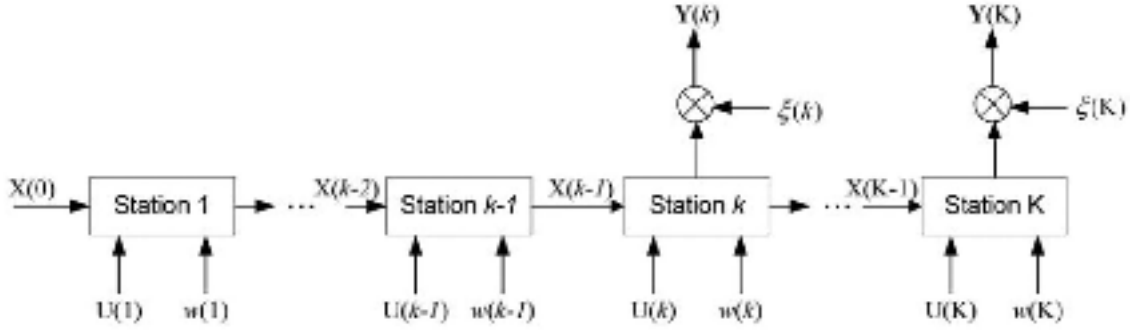

Fig. 2 Multistage manufacturing process

where n represents a white noise vector that also includes noise due to any unmodelled factors in the process. In the case of a rigid assembly, each column of the diagnostic matrix **D** represents a fault pattern related to failure of one of the KCCs, whereas in the case of a compliant assembly, the diagnostic matrix **D** is equivalent to the inverse stiffness matrix of the product [**34**]. Each column of the inverse stiffness matrix **D** represents the impact of a unit fault on deformations of the assembly structure and **Γ** is equivalent to **D** in equation (4). The inverse stiffness matrix can be developed for each assembled product, but it assumes that the internal forces are in equilibrium at any time [**25**, **48**]. In general, this requirement is satisfied while locating a part or subassembly in N–2–1 fixtures. The relationship between the external forces and displacement of a compliant part or subassembly can be defined as [**40**]

$$\mathbf{F} = \mathbf{SX} \tag{5}$$

where **F** represent external forces and $\mathbf{X} = \{x_1, x_2, \ldots, x_n\}$ represents displacement at KCCs and **S** denotes the stiffness matrix. The stiffness matrix can be condensed to the inverse stiffness matrix (**D**), which defines the relationship between external forces and displacement on KPCs

$$\mathbf{X} = \mathbf{DF} \tag{6}$$

where $\mathbf{D} = \mathbf{S}^{-1}$ and can be represented in the following form

$$\mathbf{D} = \begin{bmatrix} d_{11} & d_{12} & \cdots & d_{1m} \\ d_{21} & d_{22} & \cdots & d_{2m} \\ \vdots & \vdots & \ddots & \vdots \\ d_{n1} & d_{n2} & \cdots & d_{nm} \end{bmatrix}_{n \times m} \tag{7}$$

In summary, the assumptions present in the SOVA model, the assembly response function for variation propagation, are:

1. All parts are properly located by fixtures.
2. There are only fixture locators errors; the errors are small and none of the locating points will lose contact.
3. Locator-part points of contacts are characterized as frictionless points.

The assumptions that are present in the SOVA model and also affect the performance of EPLS methodology are:

4. The measurement noise and process noise are considered to be independent of each other.
5. Each measurement noise is considered to be independent of each other, i.e. $\sum_{\xi} = \sigma_c^2 \mathbf{I}$, where $\sum_{\xi}$ is the covariance matrix for measurement noise and σ_c^2 is the variance associated with each measurement point.
6. Measurement noise is considered to have zero mean and σ_c^2 variance at all stations.
7. Each process noise is considered to be independent of each other, i.e. $\sum_{\mathbf{w}} = \sigma_u^2 \mathbf{I}$, where $\sum_{\mathbf{w}}$ is the covariance matrix for measurement noise and σ_u^2 is the variance associated with each key control characteristic.

Assumptions 1 to 3 are requirements that must be ensured in the part and fixturing design process. Assumptions 4 to 7 are simplifications to SOVA modelling and these assumptions are also considered as a part of the assembly response function while developing the EPLS methodology.

3 ENHANCED PIECEWISE LEAST SQUARES APPROACH FOR DIAGNOSIS OF COMPLIANT ASSEMBLIES

The following section discusses the proposed enhanced piecewise least square (EPLS) methodology.

3.1 Enhanced piecewise least squares regression approach

Generally, faults in the manufacturing processes are manifested through measurement points taken at critical locations, also called the MLPs (measurement locating points) [**25**]. While measurement data indicate occurrence and patterns of dimensional variation, however, they do not directly relate to the root causes of the faults that cause these variations. In order to diagnose the fault, the variation pattern of the MLPs must be extracted from the covariance matrix of the multivariate data. Most diagnostic approaches assume that the diagnostic matrix **D** has independent columns, though this assumption does not always hold for most manufacturing processes dealing with compliant parts where the diagnostic matrix can be represented by the inverse stiffness matrix as described in section 2. Thus, the most important part in the diagnostic approach for compliant assembly is the formulation of the state vector (***X***), which must be defined in accordance with the measurements described by MLPs (**Y**). If the parameters selected while defining the state vector have less influence on the measurement then it will result in noise and will induce errors in the results, reducing the generalization capability of the model. There are many statistical approaches dealing with such problems; the partial least squares (PLS) approach is used most often for predictive linear modelling, especially with a large number of predictors. However, the PLS approach tends to overlook

the real correlation caused by high leverage outliers leading to imprecise results.

The developed EPLS method enhances the traditional PLS algorithm by overcoming the aforementioned limitations. The goal of PLS is to predict response **Y** from the state vector ***X***. When **X** is full rank, this goal is accomplished using ordinary multiple regression, whereas when **X** is likely to be singular then the regression approach is no longer feasible because of multicollinearity. Several approaches have been developed to deal with this problem. One approach is to eliminate some predictors (e.g. using stepwise methods) [**49**]. Another technique involves performing a principal component analysis (PCA) on the **X** matrix and then using these principal components of **X** as regressors on **Y** [**50**, **51**]. While the orthogonality of principal components eliminates issues related to multicollinearity, it does not, however, address the problem of choosing an optimum subset of predictors. A possible strategy is to keep only a few of the first components. However, they are chosen to explain **X** rather than **Y**; thus no direct relation exists between the predictor and response. The major limitation of PLS is overlooking real correlation and sensitivity to the relative scaling of latent vectors. In the case of a negatively ill-conditioned multistage assembly system, the PLS algorithm generally gives an imprecise solution. By contrast, the EPLS methodology integrates the CAD information with the measurement data obtained from manufacturing. The CAD information is used to transform the working plane of process variables such as fixtures from a design nominal to the lower bound of design tolerances using the SOVA model [**29**]. This transformation makes a negative correlation an infeasible solution. Thus, to identify the six-sigma fault the similarities between the response **Y** and patterns obtained based on CAD information $\mathbf{D}(i)$ is observed, which is then represented by a positive correlation. The developed EPLS regression searches for a set of components called latent vectors that performs a simultaneous decomposition of **X** and **Y** with the constraint that the latent vector ($\bar{V}$) consists of only positive correlation components to explain most of the similarity between **X** and **Y**. The decomposition of the inverse stiffness matrix **D** is done to obtain the sensitivity of each latent vector ($\bar{V}$). EPLS generates the relevant fault parameters for diagnosis, which satisfy the linear structure of the model as in equation (4). The first equation below determines the latent vector of EPLS based on the projection of response **Y** on the variation patterns of the diagnostic matrix **D** with the constraints as shown in the second equation

$$\bar{\mathbf{V}}_1 = \mathbf{D}\mathbf{C}_1 \tag{8}$$

$$\mathbf{C}_1 = \begin{cases} [C_{j1}]_{1 \le j \le m} & \text{if } C_{j1} \ge 0 \\ C_{j1} & \text{else} \end{cases} \tag{9}$$

where

$$\mathbf{C}_{j1} = \frac{[D_j - \mu_{D_j}][Y - \mu_Y]^T}{\sqrt{\sum_{j=1:m} ([D_j - \mu_{D_j}][Y - \mu_Y]^T)^2}}$$

During the assembly process, part and process variations influence the manufactured product. The compliance of parts and subassemblies may result in an ill-conditioned system causing the inverse stiffness matrix **D** to become singular. To deal with the singularity issue, the QR factorization method is applied on **D**. The inverse stiffness matrix **D** can be represented as

$$\mathbf{D} = \mathbf{Q}\mathbf{R} \tag{10}$$

where $\mathbf{R} \in \Re^{n \times m}$ is upper triangular with $r_{ii} \ge 0$ and $\mathbf{Q} \in \Re^{n \times n}$. Both **Q** and **R** are orthogonal matrices and **R** is a non-singular matrix. The elements of **D** can be represented as

$$d_{ij} = \sum_{k=1:n} q_{ik} r_{kj} \tag{11}$$

where $I = 1,2,\ldots,n$ and $j = 1,2,\ldots,m$. If $k \ge i$ then $r_{kj} = 0$, and thus equation (11) can be further reduced to

$$d_{ij} = \sum_{k=1:j} q_{ik} r_{kj} \tag{12}$$

Using the first latent vector ($\bar{V}_1$) obtained from equation (8), linear regression is performed as follows

$$\mathbf{Y} = a_1 \bar{\mathbf{V}}_1 + \mathbf{Y}^{(1)} \tag{13}$$

$$\mathbf{D} = \bar{\mathbf{V}}_1 \mathbf{b}_1 + \mathbf{D}^{(1)} = \mathbf{Q}_1 \mathbf{R}_1 \mathbf{b}_1^T + \mathbf{D}^{(1)} \tag{14}$$

where a_1 and $\mathbf{b}_1$ are regression coefficients and the regression vector respectively. Matrix $\mathbf{D}^{(1)}$ is the input residual vector and $\mathbf{Y}^{(1)}$ is output residual vector. If the residual vector $\mathbf{Y}^{(1)}$ is important, a second EPLS component $\bar{\mathbf{V}}_2$ is calculated using the following equations

$$\bar{\mathbf{V}}_2 = \mathbf{D}^{(1)}\mathbf{C}_2 \tag{15}$$

$$\mathbf{C}_2 = \begin{cases} [C_{j2}]_{1 \le j \le m} & \text{if } C_{j2} \ge 0 \\ C_{j2} & \text{else} \end{cases} \tag{16}$$

where

$$\mathbf{C}_{j2} = \frac{[D_j - \mu_{D_j}][Y^{(1)} - \mu_Y]^T}{\sqrt{\sum_{j=1:m} ([D_j - \mu_{D_j}][Y^{(1)} - \mu_{Y^{(1)}}]^T)^2}}$$

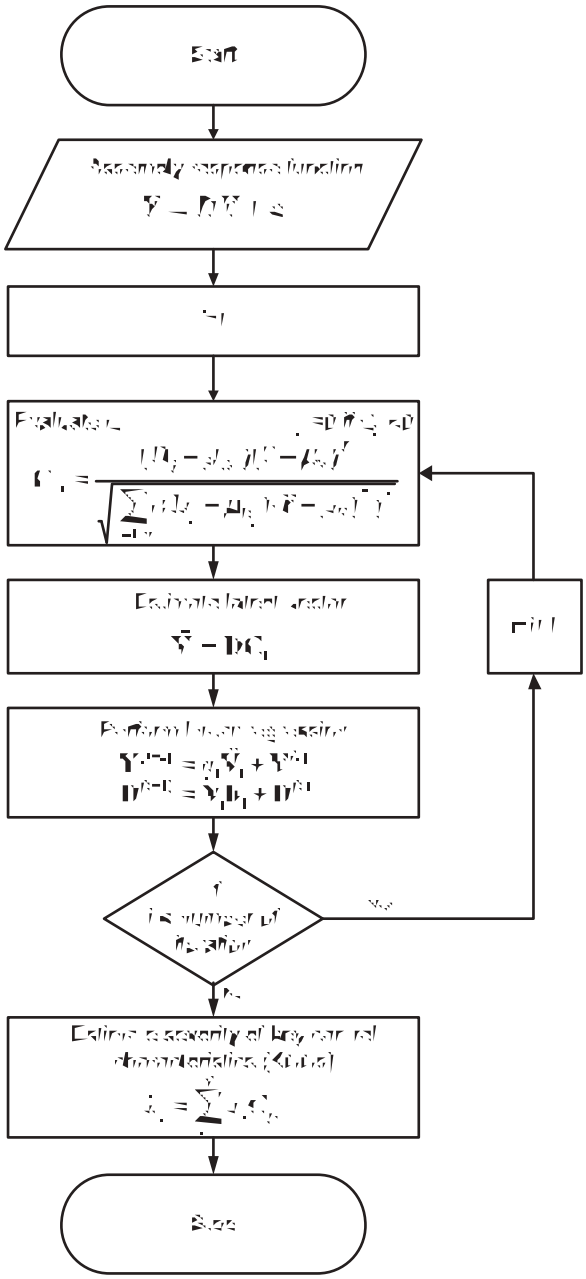

Fig. 3 Flowchart of EPLS methodology

A regression of $\mathbf{Y}$ on first latent vector ($\bar{\mathbf{V}}_1$) and second latent vector ($\bar{\mathbf{V}}_2$) is shown in the following equation

$$\mathbf{Y} = a_1\bar{\mathbf{V}}_1 + \mathbf{Y}^{[1]} = a_1\bar{\mathbf{V}}_1 + a_2\bar{\mathbf{V}}_2 + \mathbf{Y}^{[2]} \quad [17]$$

The process of regression is iterated on the residual obtained from the previous step. After S number of iterations, the SOVA assembly response model can be represented as follows, where the estimated quantity is denoted by a circumflex

$$\mathbf{Y} = \hat{\mathbf{Y}} + \xi \quad [18]$$

where $\hat{\mathbf{Y}} = :V$, $\mathbf{V} = [\bar{V}_1 \bar{V}_2 \ldots \bar{V}_s]$, and $:= [a_1\ a_2 \ldots a_s]^T$, and S is the total number of iterations. The flowchart of EPLS methodology is shown in Fig. 3.

The number of iterations for the EPLS approach can be decided based on experimentation using different criteria, such as the normalized mean square error (NMSE), mean square error (MSE), residual square (R^2), adjusted coefficient of multiple determination ($AjdR^2$), Akaike information criterion (AIC), Hannan and Quinn information criterion (HQ), and the Bayesian information criterion [**52**]. In this research, an MSE criterion is used to set the number of iterations in the EPLS approach. The MSE criterion represents the mean variation in error and is represented as

$$MSE = \frac{\sum_{i=1}^{N} [y_i - \hat{y}_i]^2}{N}$$

Remarks

1. *The proposed EPLS method is general for the system that can be represented as a linear assembly response function, for example the SOVA model.*
2. *The advantage of the proposed EPLS approach as compared to PLS is that it identifies the real correlation between the state vector* $\mathbf{X}$ *and response* $\mathbf{Y}$ *considering the linear assembly response function, for example the SOVA model represented in the form of the* $\mathbf{D}$ *matrix.*

3.2 Performance evaluation

The latent vector ($\bar{V}$) of EPLS can be interpreted as capturing variations having a positive correlation with the observation $\mathbf{Y}$. The EPLS approach removes irrelevant information from the response vector to identify the best possible faults in the case of an ill-conditioned system. Let $\{a_s\}$ denote the variation captured by the latent vector $\bar{V}_s$ for response $\mathbf{Y}^{(s-1)}$, where $s = 1, 2, \ldots, S$, and $\mathbf{Y}$ is the actual measurement. Matrix $:[\cdot]$ contains variations captured by each latent vector $\mathbf{V}[\cdot]$. Thus, $\{a_s\}$ is, in some sense, the measure of sensitivity of each latent vector to a given response $\mathbf{Y}$ and $\{b_{js}\}$ represents the sensitivity of the jth fault parameter $\hat{x}_j$ with respect to the latent vector $\bar{\mathbf{V}}_s$. C_{js} measures the linear association between the response $\mathbf{Y}$ and diagnostic vectors $\mathbf{D}$; thus it can be interpreted as the contribution of pattern j in the *latent vector* $\bar{\mathbf{V}}_s$. In the case where C_{js} is negative, then C_{js} has a negative association with $\mathbf{Y}^{(s-1)}$; thus it is set to zero to eliminate the effect of the j column from $\mathbf{D}$ while evaluating the latent

vector. The measure of severity of fault can be estimated by using

$$\hat{x}_j = \sum_{s=1}^{S} a_s C_{js} \tag{19}$$

where $\hat{\mathbf{X}} = [\hat{x}_1 \hat{x}_2 \ldots \hat{x}_m]$ is the severity of faults. When $\hat{x}_j$ is equal to zero this shows that there is no deviation from the nominal or the jth locator has no contribution in the response $\mathbf{Y}$, whereas, on the other hand, if $\hat{x}_j$ has a large magnitude this means that the fault is very severe. This interpretation has been used to estimate the faults. If the estimated magnitude of $\hat{x}_j$ is larger than some predicted threshold value then it is concluded that jth faults are present. The prediction threshold can be set either based on KCC tolerances as defined in the design or it can be determined experimentally based on simulations using a process model such as SOVA. The second approach helps to include the process noise, if any, while setting up the fault alarm threshold. The variance associated with estimated KCCs (key control characteristics) can be determined using

$$\hat{\sigma}_j^2 = \frac{1}{N} \sum_{j=1}^{m} \hat{x}_j^2 \tag{20}$$

A fault can be uniquely determined if the projection of each variation pattern of the diagnostic matrix $\mathbf{D}$ on response $\mathbf{Y}$ can be uniquely represented

$$Q_i = (\mathbf{D}_j - \mu_{\mathbf{D}_j})(\mathbf{Y}^l - \mu_{\mathbf{Y}^l})^T \tag{21}$$

where $j = 1, 2, \ldots, n$ represents the columns of the inverse stiffness matrix and $l = 1, 2, \ldots, L$, where L is the number of latent variables used in the predictions.

The unmodelled noise present in the system has an impact on the performance of the algorithm. Thus, proper treatment with a dataset is needed to deal with the unmodelled noise present in the system.

If the model has a variable variance E, with each KCC represented as $E = \text{diag}\{\sigma_1^2 \sigma_2^2 \ldots \sigma_n^2\}$, then it will lead to a biased solution. Let E be the error component of the response that can be estimated using

$$\hat{E}^2 = E\{|\mathbf{DX} - \mathbf{bY}|^2\} \tag{22}$$

where $\mathbf{b} = (\mathbf{D}^T\mathbf{D})^{-1}\mathbf{D}^T\mathbf{Y}$. Assuming that the response $\mathbf{Y}$ and noise E are uncorrelated, equation (22) can be reduced to

$$\begin{aligned} \hat{E}^2 &= E\{|\mathbf{DX} - \mathbf{b}(\mathbf{DX} + E)|^2\} \\ &= E\{|(\mathbf{I} - \mathbf{b})\mathbf{DX}|^2\} + E\{|\mathbf{b}E|^2\} \end{aligned} \tag{23}$$

where $E\{|\mathbf{b}E|^2\}$ is the variance due to noise and $E\{|(\mathbf{I} - \mathbf{b})\mathbf{DX}|^2\}$ is the biased squared signal error.

To make noise independently identically distributed (i.i.d.) and uncorrelated in the above situation the response $\mathbf{Y}$ is multiplied by the weights $\mathbf{W}$, where

$$W = (\hat{E}\hat{E}^T)^{-1} = \begin{bmatrix} \sigma_1^2 & 0 & 0 & 0 \\ 0 & \sigma_2^2 & 0 & 0 \\ 0 & 0 & \ldots & 0 \\ 0 & 0 & 0 & \sigma_n^2 \end{bmatrix}^{-1}$$

The $\mathbf{W}$ can be estimated using the data from the production when none of the faults is present. The $\mathbf{W}$ helps in minimizing the sum squares of residual as follows

$$\min_X (\mathbf{Y} - \hat{\mathbf{Y}})^{\mathrm{T}} \mathbf{W}^{-1} (\mathbf{Y} - \hat{\mathbf{Y}}) \tag{24}$$

Solving equation (24) gives

$$\min_X (\mathbf{Y}' - \hat{\mathbf{Y}}')^T (\mathbf{Y}' - \hat{\mathbf{Y}}') \tag{25}$$

where $\mathbf{Y}' = \mathbf{W}^{-1/2}\mathbf{Y}$, $\hat{\mathbf{Y}}' = \mathbf{W}^{-1/2}\mathbf{DX}$, and $E' = \mathbf{W}^{-1/2}E$. Thus, equation (18) can be rewritten as

$$\mathbf{Y}' = \hat{\mathbf{Y}}' + E \tag{26}$$

Using the adjusted values, the noise in the system can be converted into i.i.d. and uncorrelated, as follows

$$E\{E'E'T\} = E\{\mathbf{W}^{-1/2}EE^T\mathbf{W}^{-1/2}\} = \mathbf{W}^{-1/2}\mathbf{W}\mathbf{W}^{-1/2} = \mathbf{I} \tag{27}$$

Thus, the noise during simulation is considered to be uncorrelated and to follow the normal distribution $E' \sim \mathrm{N}[0, \sigma_E]$ with the same variance at each station, and also considering that σ_E and σ_s are the variances of the error and signal respectively. The affect of noise in the system is evaluated through the signal-to-noise ratio, which can be defined as the ratio between the signal-to-noise variance as

$$S_n = \frac{\sigma_s^2}{\sigma_E^2} \tag{28}$$

where S_n is the signal-to-noise ratio, σ_s^2 is the variance of n measurement points, and σ_E^2 is the variance due to unmodelled factors. The signal variance can be evaluated using

$$\hat{\sigma}_s = \frac{S}{C_4} \tag{29}$$

where

$$C_4 = \frac{4(N-1)}{4N-3}$$

N is number of samples used to estimate the deviation, and

$$S = \frac{\sum_{i=1}^{N} S}{N} \tag{30}$$

where S is the average variance at all KPCs and S is the variance of the measurement point for each KPC considering N samples. The variance in the signal due to noise is estimated as

$$\hat{\sigma}_E^2 = \frac{1}{N(n-m)} \sum_{j=1}^{N} \hat{e}\hat{e}^T \tag{31}$$

where

$$\hat{e} = \mathbf{Y} - \hat{\mathbf{Y}} = \mathbf{Y} - \sum_{i=1}^{S} a_i \mathbf{V}_i$$

For the signal fault case the fault alarm can be generated based on the threshold limit, where the threshold limit to generate the fault alarm for the current problem has been estimated using Monte Carlo simulation. From the estimated value of $\hat{x}_i$, $\hat{\sigma}_i$ has been evaluated using equation (20) where $i = 1, 2, \ldots, m$ and the $2\hat{\sigma}_i$ limit has been used as a threshold limit for generating the fault alarm for every KCC. The $2\hat{\sigma}_i$ limit represents the 95 per cent confidence interval associated with variations of KCCs assuming that the KCCs follow the Gaussian distribution.

4 SIMULATION TESTING AND RESULTS

The proposed methodology is tested on a five-stage multistation assembly process with compliant parts as shown in Fig. 4. The model has 14 KCCs and 65 KPCs, whose relations are modelled with 87 beam elements. For every beam element, the stiffness information parameter is defined as follows: the product material is referred to steel characteristics; the inertia moments $\mathbf{I}_{yy}$ and $\mathbf{I}_{zz}$ and cross-section area are calculated according to the three different types of beam shapes (□shape, U shape, and L shape); and the assembly process consists of five operations, conducted in five stations, where the following parts are assembled: right door frame, left door frame, front bow, central bow, and rear bow, which are assembled in stations 1 to 5 respectively.

The inverse stiffness matrix obtained from the ANSYS finite element simulation software is used to simulate different fault scenarios with noise in the assembly system. The different KCCs considered while building the ANSYS model are shown in Fig. 5.

The proposed methodology is discussed for single- and two-fault scenarios.

4.1 Single-fault scenario

This section analyses the assembly system diagnosability in the single-fault scenario. The inverse stiffness

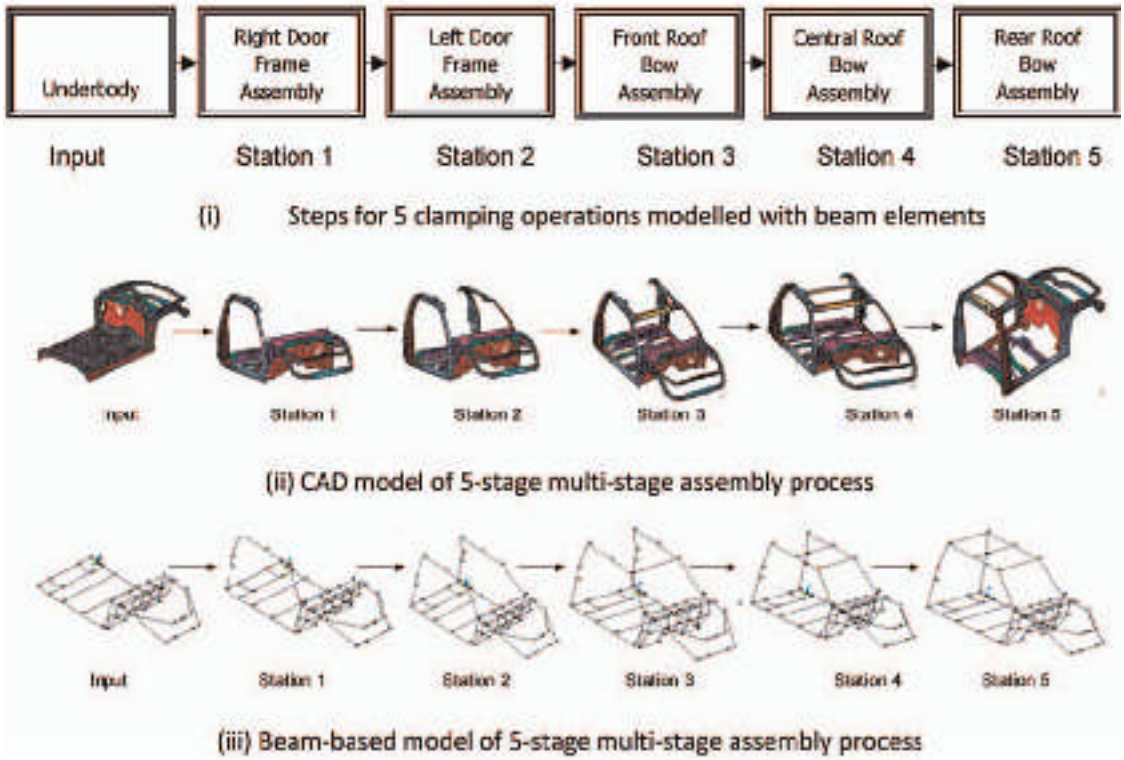

Fig. 4 Assembly process of beam-based model occurring at five stations

matrix ($\mathbf{D} \in \mathbb{R}^{195\times14}$) obtained from simulation is singular and has rank 7. To deal with the singularity in the inverse stiffness matrix **D** while performing a least squares estimation as shown in equation (14), QR factorization is used. **Q** obtained from QR factorization is a full rank orthogonal matrix (i.e. $\mathbf{Q}^{\mathrm{T}}\mathbf{Q} = \mathbf{I}$) with dimension 195×195 and **R** is an upper triangular with dimension 195×14, an example of **Q** and **R** obtained for the five-stage multistation assembly model as given in Table 2.

The diagnosibility of a fault in a multistage assembly system depends on several factors, such as the position in the assembly process, magnitude of variation, and signal-to-noise ratio (S/N). In the proposed method only the mean and variance of the process fault are considered for fault isolation. Equation (31) is used to assign weights to each variation pattern. A negative value of Q_i for ith latent variables is set to zero to tackle negative collinearity in the system. Q_i obtained for the single-fault case for all latent variables is given in Table 3.

The effectiveness of the EPLS has been estimated for single faults by carrying out simulations on the above-mentioned beam-based assembly model. The EPLS capability to capture the variation of the data depends on the number of latent variables defined. To decide on the number of latent variables needed to capture the variation in the case of single faults,

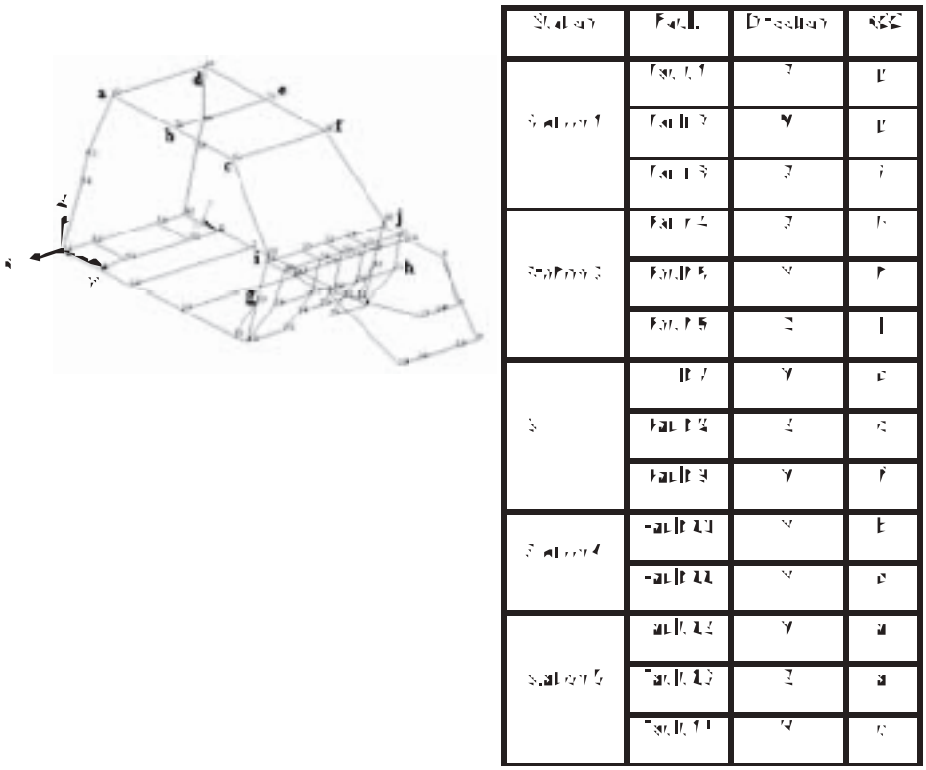

Fig. 5 KCCs considered for a beam model for fault failure

Table 2 R matrix obtained from stiffness matrix

2.502	2.502	2.035	2.035	0.001	0.001	0.001	0.001	0.077	0.077	0.141	0.141	0.176	0.176
0.000	0.000	0.043	0.043	0.003	0.003	0.002	0.002	0.002	0.002	0.019	0.019	0.013	0.013
0.000	0.000	1.611	1.611	0.007	0.007	0.021	0.021	0.298	0.298	0.548	0.548	0.573	0.573
0.000	0.000	0.000	0.000	0.025	0.025	0.019	0.019	0.031	0.031	0.052	0.052	0.090	0.090
0.000	0.000	0.000	0.000	1.180	1.180	0.205	0.205	0.106	0.106	0.161	0.161	0.147	0.147
0.000	0.000	0.000	0.000	0.000	0.000	0.009	0.009	0.105	0.105	0.201	0.201	0.172	0.172
0.000	0.000	0.000	0.000	0.000	0.000	1.331	1.331	0.031	0.031	0.053	0.053	0.077	0.077
0.000	0.000	0.000	0.000	0.000	0.000	0.000	0.000	0.013	0.013	0.023	0.023	0.024	0.024
0.000	0.000	0.000	0.000	0.000	0.000	0.000	0.000	2.364	2.364	3.397	3.397	3.690	3.690
0.000	0.000	0.000	0.000	0.000	0.000	0.000	0.000	0.000	0.000	0.025	0.025	0.045	0.045
0.000	0.000	0.000	0.000	0.000	0.000	0.000	0.000	0.000	0.000	1.864	1.864	0.082	0.082
0.000	0.000	0.000	0.000	0.000	0.000	0.000	0.000	0.000	0.000	0.000	0.000	0.114	0.114
0.000	0.000	0.000	0.000	0.000	0.000	0.000	0.000	0.000	0.000	0.000	0.000	-1.004	1.004
zero(183 x 14)													

extensive experimentation at a different number of iterations was carried out for each fault; the iterations with a minimum average MSE for the entire fault were taken as the threshold for the number of iterations, as shown in Figs 6 to 8.

From Figs 6 to 8, it can be observed that EPLS captured most of the variations, with 10 latent variables for all the fault cases. As the variations captured by higher latent variables are negligible, the number of latent variables is set to 10. Figure 9 shows the fitting obtained by 10 latent variables against the actual measurement **Y**.

The EPLS was tested on several simulated faults and sensitivity ($\ddot{x}_j$) has been used to evaluate the faults. The $2\ddot{\sigma}_i$ limit is set as the fault alarm threshold for KCC_i. The selection of sample sizes to have a correct estimate of the fault is an important issue; thus simulations have been carried out considering failure of KCC 4 in the system using a sample size of 30. Fault KCC 4 has a high positive correlation of 0.7861 with KCC 2 and a negative correlation of −0.7861 and −1.0 with KCCs 1 and 3 respectively. The EPLS algorithm stops either when the number of latent vector reaches 10 or when there is no positive association of the column vector from **D** to response **Y**, which is used to terminate the algorithm. The simulation results have been shown in Fig. 10.

From Fig. 10 it can be seen that the solution becomes stable with increasing sample size. The EPLS methodology is compared with the classical PLS for a common dataset with the same parameters and the results are shown in Figs 11 and 12.

Table 3 C_j obtained for different latent variables

	Latent variables									
X	1	2	3	4	5	6	7	8	9	10
1	0.3052	0.5162	0.0307	0	0	0.1424	0	0	0	0
2	0	0	0	0.3838	0	0.4645	0	0.603	0	0.8585
3	0.3027	0.6183	0.1249	0.0076	0	0.2498	0	0	0	0
4	0	0	0	0.2913	0	0	0	0	0	0
5	0.0159	0.0497	0.0834	0.0044	0.0596	0.0009	0.287	0	0.2702	0.5128
6	0	0	0	0	0.1572	0	0.1148	0.1295	0.8174	0.0002
7	0.1321	0.3874	0.5353	0.7117	0.3497	0	0	0	0	0
8	0	0	0	0	0	0	0	0	0	0
9	0.3654	0	0	0.189	0.4937	0.3621	0.8696	0	0.0852	0
10	0	0.1506	0	0	0	0	0	0	0	0
11	0	0.287	0.0837	0.4289	0.5913	0.7553	0.357	0.7872	0.5015	0
12	0.5759	0	0.8264	0	0	0	0	0	0	0
13	0.5765	0	0	0.2037	0.506	0	0.1444	0	0	0
14	0	0.3059	0	0	0	0	0	0	0	0

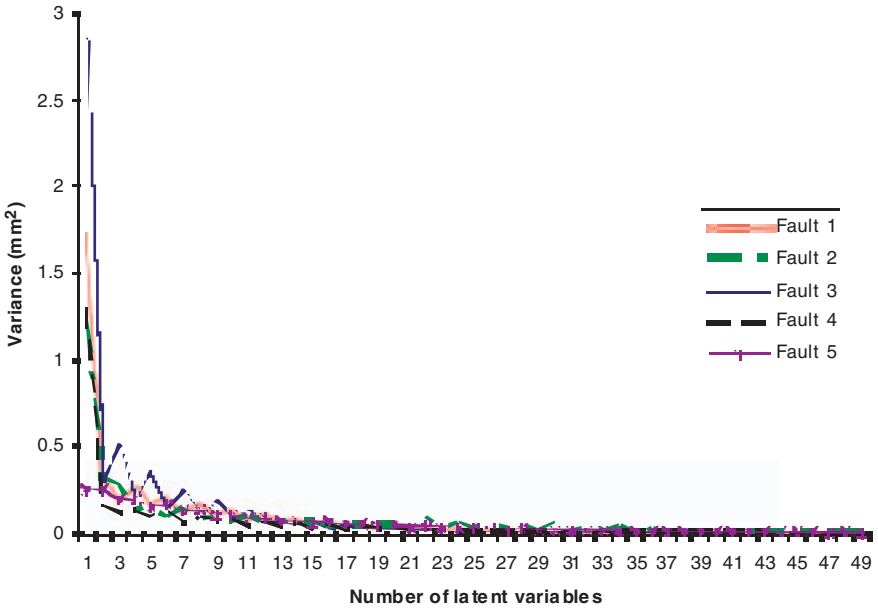

Fig. 6 Variations resulting from different latent variables for a single-fault scenario for faults 1 to 5

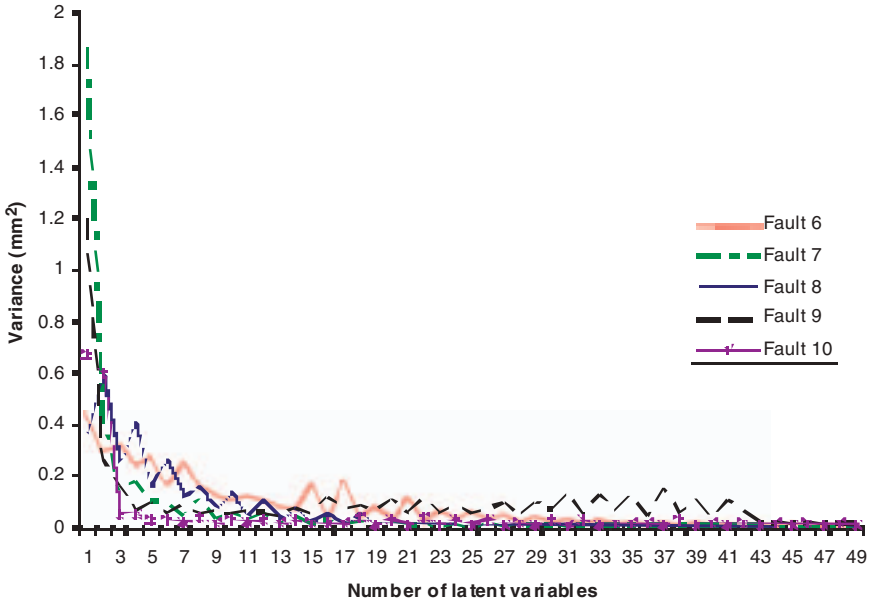

Fig. 7 Variations resulting from different latent variables for a single-fault scenario for faults 6 to 10

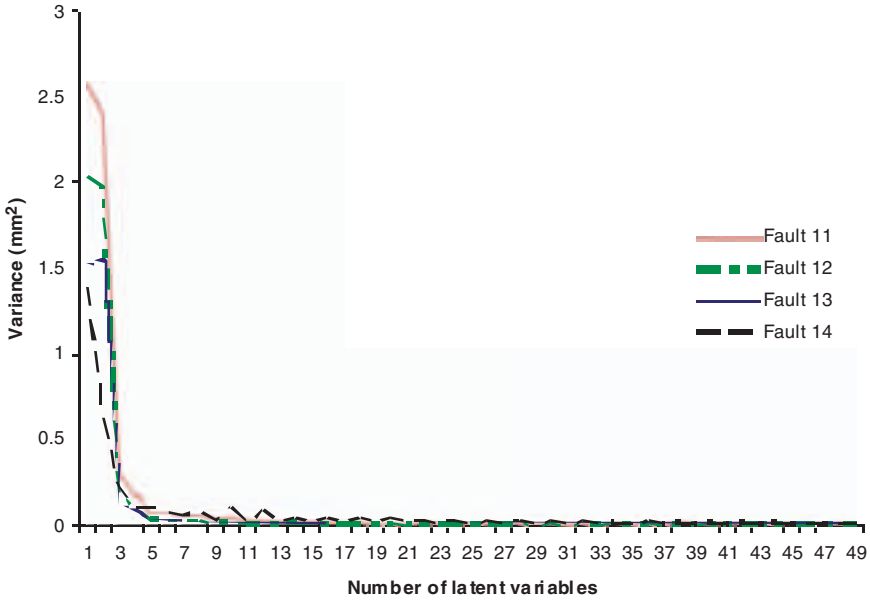

Fig. 8 Variations resulting from different latent variables for a single-fault scenario for faults 11 to 14

From Fig. 11 it can be seen that the PLS assigns the same magnitude for negatively collinear faults, which thus cannot be identified, whereas Fig. 12 is based on constraining the latent vector by the assembly response function, the SOVA model of the assembly system, by performing decomposition on response (end-of-line-measurement).

Monte Carlo simulation has been carried out to estimate the operating characteristic curve (OC curve) or Type-II error for different faults with varying signal-to-noise ratios. The OC curve obtained for faults detection has been plotted with respect to different signal-to-noise ratios, as shown in Fig. 12. The Type-II error obtained from EPLS has been compared with the least squares (LS) estimation approach; the comparison is shown in Fig. 13.

From Fig. 13, the comparison of diagnostic performance of EPLS with LS for the Type-II error indicates that LS is unable to diagnose the fault in most of the cases of moderate signal-to-noise ratios, whereas EPLS is able to diagnose the fault effectively in a noisy assembly environment.

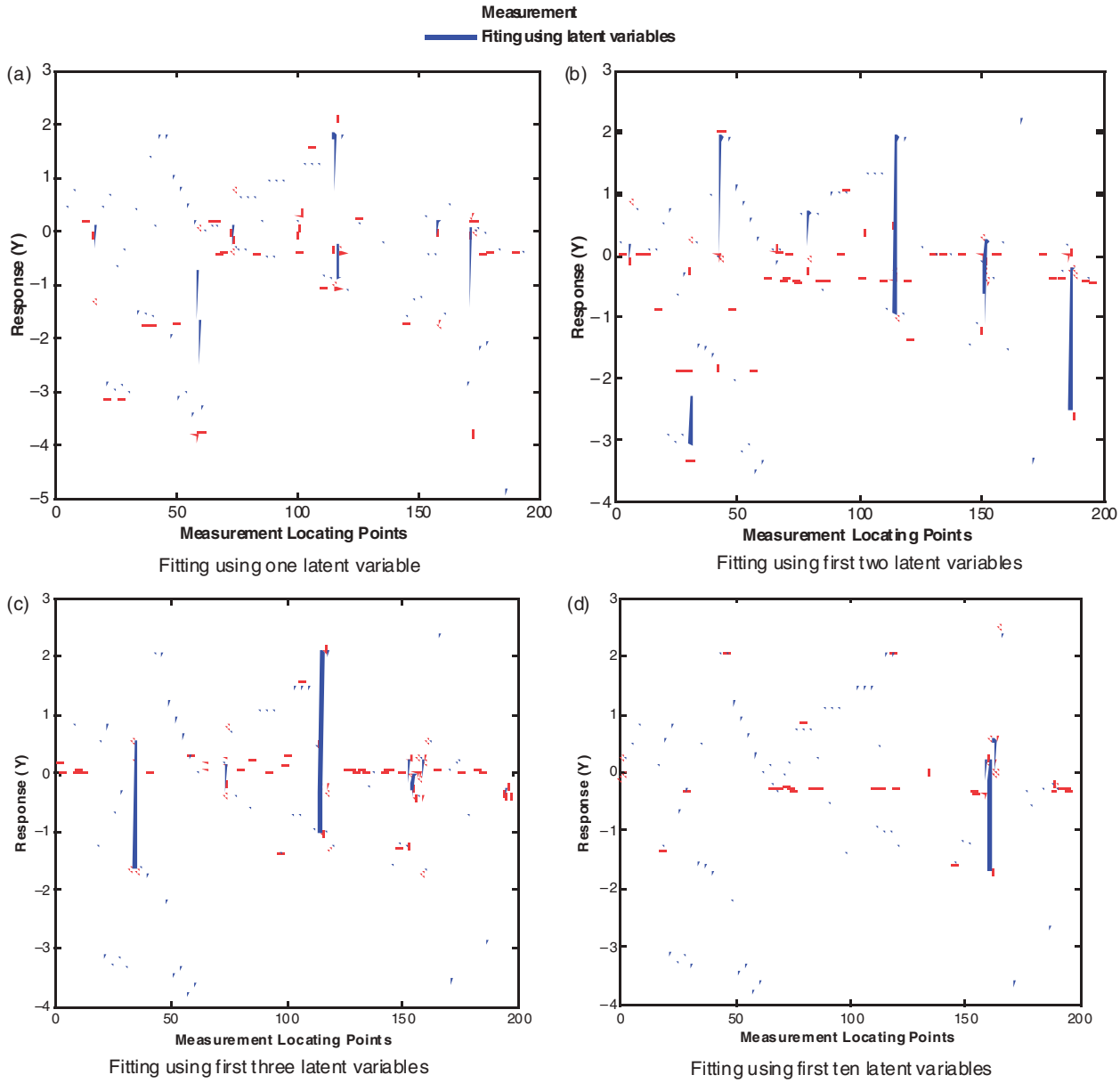

Fig. 9 Fitting capability of EPLS

4.2 Two faults in the system

This section discusses the diagnosibility of EPLS when two faults occur simultaneously in the system. The effect of sample size on the sensitivity estimation using the EPLS algorithm has been studied for two different fault scenarios of independent faults and highly correlated faults. The EPLS algorithm is run for independent samples with a sample size of 30. The results obtained are shown in Figs 14 and 15.

Further, in order to understand the effect of collinearity on the diagnosability performance of EPLS, Monte Carlo simulation has been performed to evaluate the Type-II error for different sets of faults and with varying signal-to-noise ratios from 0 to 3.0 and fault magnitude ratios varying from 0.1 to 1.0. The results obtained are shown in the form of an OC surface instead of an OC curve, as shown in Fig. 16.

The computational time required to obtain Fig. 16 is estimated to be 96 hours on a Dell PC with a 2.8 GHz Pentium processor. Figure 16 demonstrates that, when there are two faults in the multistage assembly system, the effect of magnitude has a greater impact on the diagnosability than the signal-to-noise ratio while operating in a stable zone of the signal-to-noise ratio. Also, the diagnosability of the fault is maximum when the faults in the system have nearly the same magnitude, i.e. the magnitude ratio is approximately equal to one. The performance of EPLS towards multiple failures with differences in the

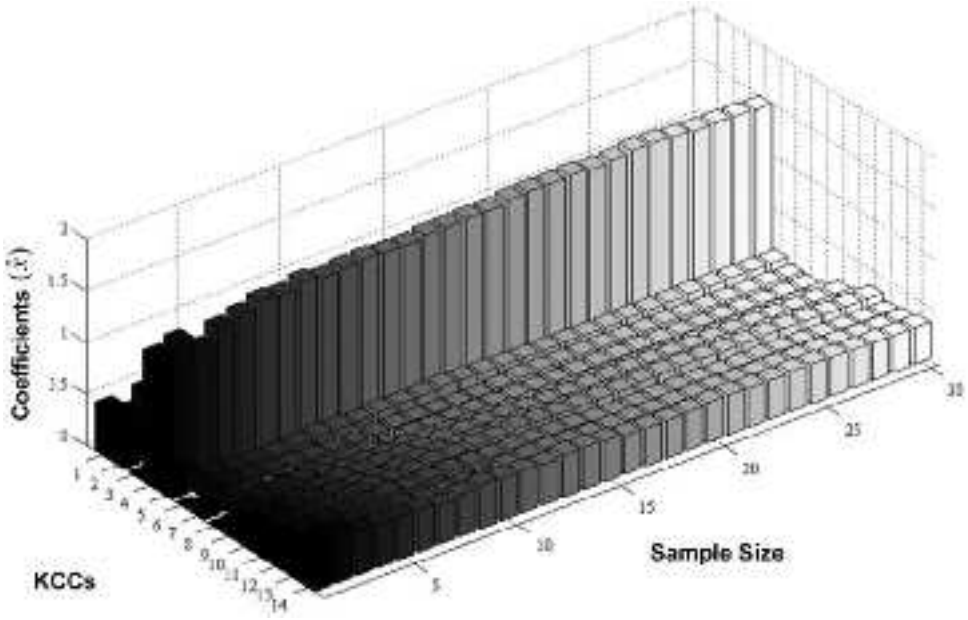

Fig. 10 Effect of sample size on accuracy in the case of a single-fault failure

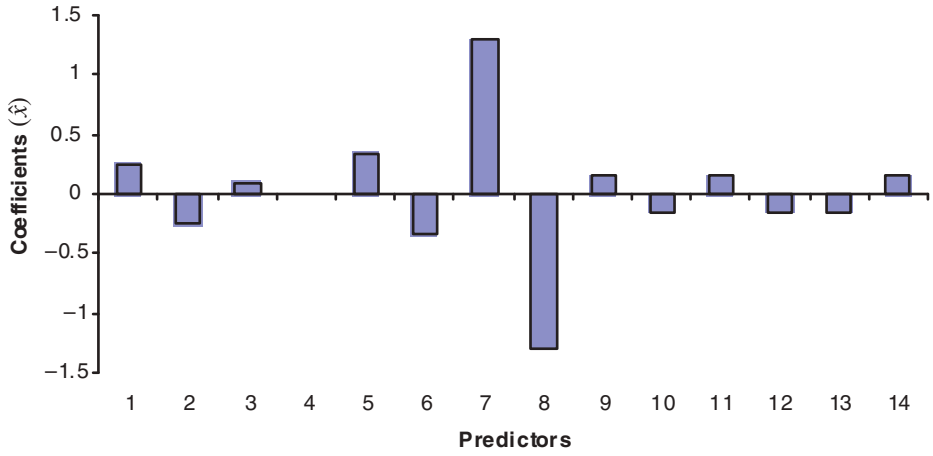

Fig. 11 Coefficients obtained using classical PLS

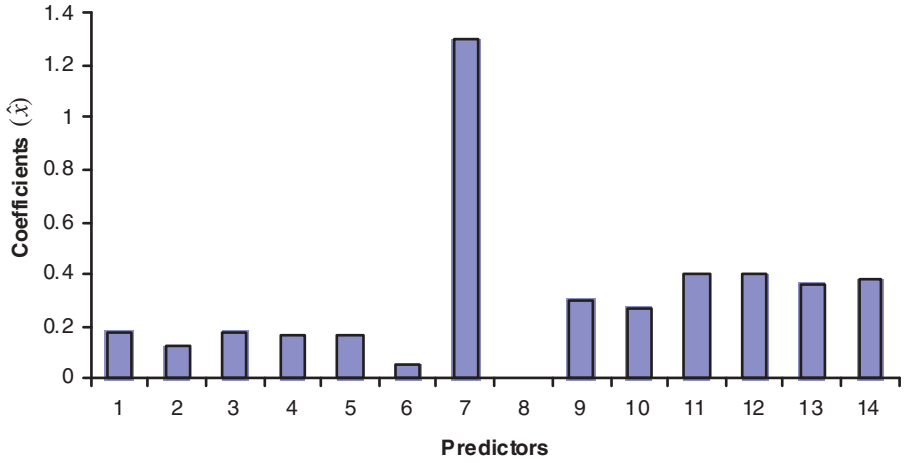

Fig. 12 Results obtained using EPLS

magnitude can be improved by including a fault pattern of a multiple fault scenario into the design matrix using an assembly response function (SOVA).

5 CONCLUSIONS

This work presents a new enhanced piecewise least squares (EPLS) methodology to diagnose fixture fault failure in an ill-conditioned multistage assembly system with compliant parts. The methodology considers the assembly response function – the stream of variation analysis (SOVA) – which can be ill-conditioned due to the compliant characteristics of the assembled product, which causes non-additive propagation of the dimensional faults. The proposed EPLS allows multiple fault predictive models to be constructed for ill-conditioned multistation assembly systems by extracting those latent vectors that account for meaningful variation by constraining each latent vector based on an assembly response function model, the SOVA model. The verification of the proposed method is presented through a series of computer simulations demonstrated for single-fault and two-fault cases. For single-fault cases, diagnosability of the fault is mostly affected by the signal-to-noise ratio whereas, in two-fault cases, diagnosability is affected more by the fault magnitude ratio than the signal-to-noise ratio.

The proposed EPLS methodology is compared with the partial least squares estimation for the single-fault scenario. Also, an extensive comparison of EPLS is carried out using state-of-the-art least squares methodology. Both of these methodologies are unable to detect the faults in ill-conditioned scenarios. The case study conducted in this paper shows that the proposed EPLS methodology is quite robust to diagnose the single-fault failure in a noisy ill-conditioned assembly system. It should be noted that future research is still needed to generalize the methodology for detecting multiple faults that are nearly collinear with nearly the same magnitude.

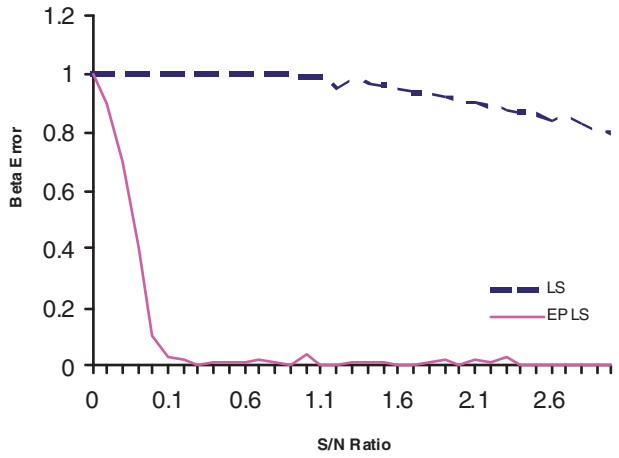

Fig. 13 Comparison of OC curves for a single-fault failure obtained using LS and EPLS

FUNDING

This research received no specific grant from any funding agency in the public, commercial, or not-for-profit sectors.

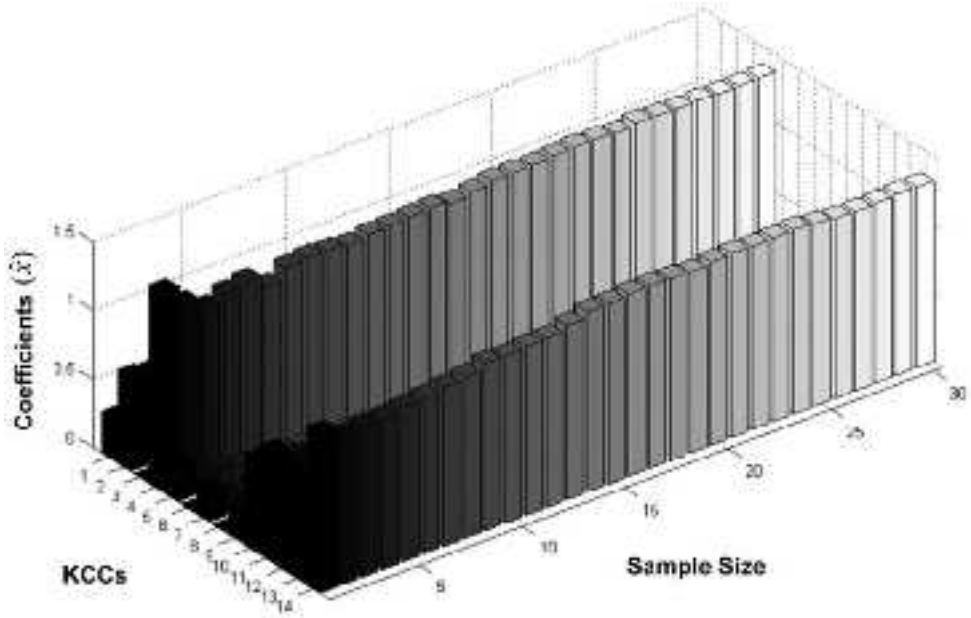

Fig. 14 Effect of sample size on accuracy in the case of two independent faults

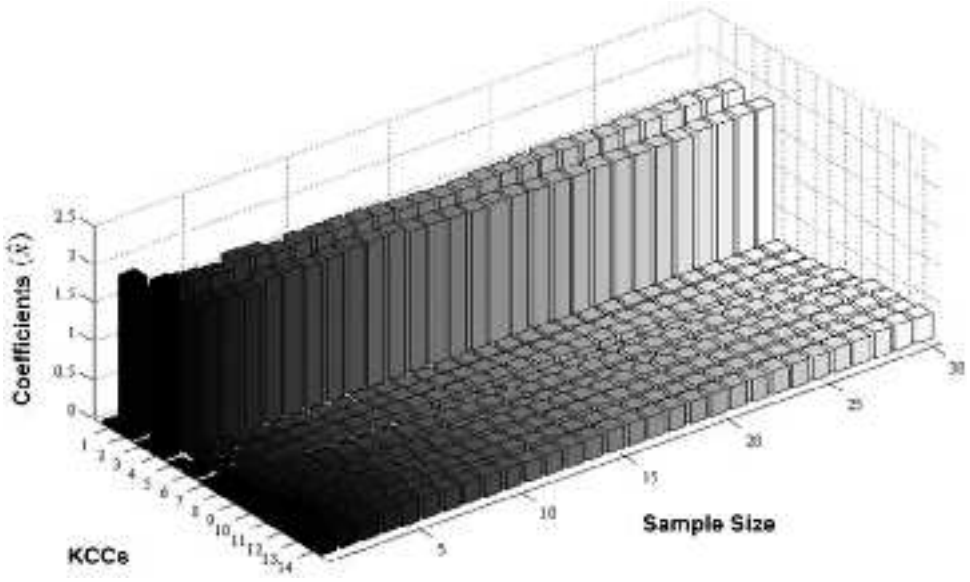

Fig. 15 Effect of sample size on accuracy in the case of two highly correlated faults

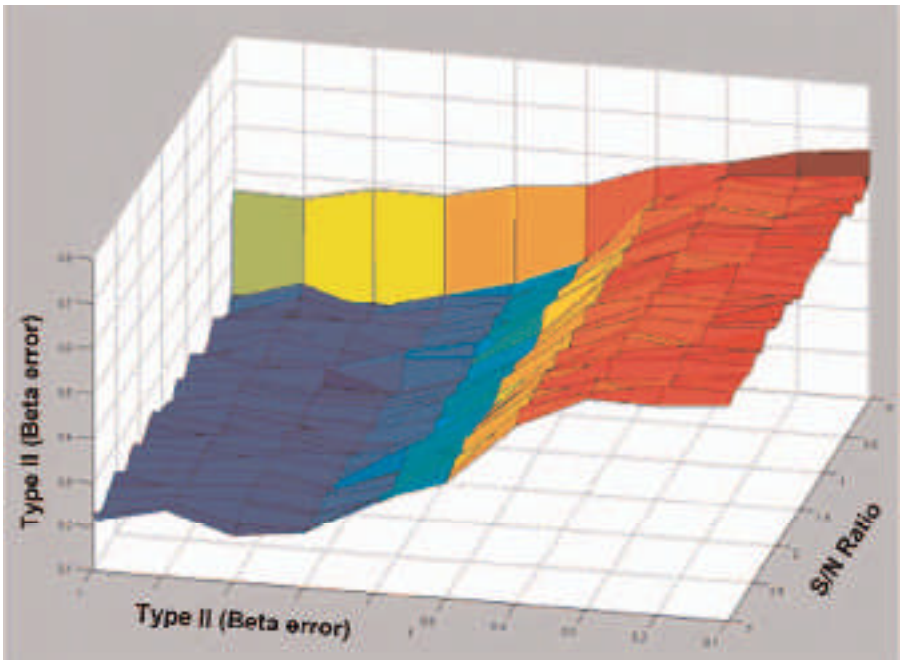

Fig. 16 OC surface obtained for two faults using EPLS

ACKNOWLEDGEMENTS

The authors gratefully acknowledge Atul Tripathi, Senior Process Improvement Engineer at National Oilwell Varco, US, and Dr Zhenyu (James) Kong, Assistant Professor at Oklahoma State University, US, for their support and assistance with this study.

REFERENCES

1 **Shalon, D., Gossard, D., Ulrich, K.,** and **Fitzpatrick, D.** Representing geometric variations in complex structural assemblies on CAD systems. In Proceedings of the 19th Annual ASME Advances in Design Automation Conference, 1992, vol. DE-44-2, pp. 121–132.

2 **Shiu, B. W., Ceglarek, D.,** and **Shi, J.** Flexible beam-based modeling of sheet metal assembly for dimensional control. *Trans. NAMR/SME*, 1997, **XXV**, 49–54.

3 **Shiu, B. W., Apley, D., Ceglarek, D.,** and **Shi, J.** Tolerance allocation for sheet metal assembly using beam-based model. *Trans. IIE, Design and Manufacturing*, 2003, **35**(4), 329–342.

4 **Asada, H.** and **By, A. B.** Kinematic analysis of workpart fixturing for flexible assembly with automatically reconfigurable fixture. *IEEE Trans. on Robot. Automn*, 1985, **RA-1**, 86–94.

5 **Ferreira, P. M., Kochar, B., Liu, C. R.,** and **Chandru, V.** AIFIX: an expert system approach to fixture design. In Proceedings of the ASME Winter Annual Meeting on *Computer-aided/intelligent process planning*, 1985, Miami Beach, Florida, pp. 73–82.

6 **Chou, Y. C., Chandru, V.,** and **Barash, M. M.** A mathematical approach to automatic configuration of machining fixtures: analysis and synthesis. *Trans. ASME, J. Manuf. Sci. Engng*, 1989, **111**(1), 299–306.

7 **Wang, M. Y.** and **Pelinescu, D. M.** Optimizing fixture layout in a point-set domain. *IEEE Trans. on Robot. Automn*, 2001, **17**(3), 312–323.

8 **Choubey, A. M., Prakash, PKS, Chan, F. T. S.,** and **Tiwari, M. K.** Solving a fixture configuration design problem using genetic algorithm with learning automata approach. *Int. J. Production Res.*, 2005, **43**(22), 412–418.

9 **Ceglarek, D., Shi, J.,** and **Wu, S. M.** A knowledge-based diagnosis approach for the launch of the auto-body assembly process. *Trans. ASME, J. Engng Industry*, 1994, **116**(4), 491–499.

10 **Ceglarek, D.** and **Shi, J.** Dimensional variation reduction for automotive body assembly. *Mfg Rev.*, 1995, **8**(2), 139–154.

11 **Zhou, S., Huang, Q.,** and **Shi, J.** State-space modeling for dimensional monitoring of multistage machining process using differential motion vector. *IEEE Trans. on Robot. Automn*, 2003, **19**(2), 296–308.

12 **Ceglarek, D.** and **Shi, J.** Fixture failure diagnosis for autobody assembly using pattern recognition. *Trans. ASME, J. Engng Industry*, 1996, **118**(1), 55–66.

13 **Rong, Y., Li, W.,** and **Bai, Y.** Locating error analysis for fixturing accuracy verification. In Proceedings of ASME Conference on *Computers in engineering*, 17–21 September 1995, Boston, Massachusetts, pp. 825–832.

14 **Rong, Y.** and **Bai, Y.** Machining accuracy analysis for computer-aided fixture design and verification. *Trans. ASME, Manuf. Sci. Engng*, 1996, **118**(8), 289–300.

15 **Jin, J.** and **Shi, J.** State space modeling of sheet metal assembly for dimensional control. *Trans. ASME, J. Manuf. Sci. Engng*, 1999, **121**(4), 756–762.

16 **Ding, Y., Ceglarek, D.,** and **Shi, J.** Modeling and diagnosis of multistage manufacturing process. Part I: state space model. In Proceedings of the 2000 Japan–USA Symposium on *Flexible automation*, 23–26 July 2000, Ann Arbor, Michigan, pp. 13146–13154.

17 **Huang, Q.** and **Shi, J.** Part dimensional error and its propagation modeling in multi-operational machining processes. *Trans. ASME, J. Manuf. Sci. Engng*, 2003, **125**(2), 255–262.

18 **Huang, Q.** and **Shi, J.** Stream of variation modeling and analysis of multistage systems serial–parallel manufacturing. *Trans. ASME, J. Manuf. Sci. Engng*, 2004, **126**(3), 611–618.

19 **Shiu, B., Ceglarek, D.,** and **Shi, J.** Multi-station sheet metal assembly modeling and diagnostic. *Trans. NAMRI/SME*, 1996, **24**, 199–204.

20 **Chang, M. H.** and **Gossard, D. C.** Modeling the assembly of compliant, non-ideal parts. *Computer-Aided Des.*, 1997, **29**(10), 701–708.

21 **Apley, D.** and **Shi, J.** Diagnosis of multiple fixture faults in panel assembly. *Trans. ASME, J. Manuf. Sci. Engng*, 1998, **120**(4), 793–801.

22 **Menassa, R.** and **DeVries, W. R.** Optimization methods applied to selecting support positions in fixture design. *Trans. ASME, Engng Industry*, 1991, **113**(4), 412–418.

23 **Cai, W., Hu, S. J.,** and **Yuan, J. X.** Deformable sheet metal fixturing: principles, algorithm and simulations. *Trans. ASME, J. Manuf. Sci. Engng*, 1996, **118**(3), 318–324.

24 **Sayeed, Q. A.** and **De Meter, E. C.** Mixed integer programming model for fixture layout optimization. *Trans. ASME, J. Manuf. Sci. Engng*, 1999, **121**(4), 701–708.

25 **Liu, S. C.** and **Hu, S. J.** Variation simulation for deformable sheet metal assemblies using finite element methods. *Trans. ASME, J. Manuf. Sci. Engng*, 1997, **119**, 368–374.

26 **Camelio, J. A.** and **Hu, S. J.** Multiple fault diagonosis for sheet metal fixtures using designated component analysis. *Trans. ASME, J. Manuf. Sci. Engng*, 2004, **126**(1), 91–97.

27 **Liu, Y. G.** and **Hu, S. J.** Assembly fixture fault diagnosis using designated component analysis. *Trans. ASME, J. Manuf. Sci. Engng*, 2005, **127**(2), 358–368.

28 **Xiong, C., Rong, Y., Koganti, R., Zaluzec, M.,** and **Wang, N.** Geometric variation prediction in automotive assembly. *Assembly Automat. J.*, 2002, **22**, 260–269.

29 **Camelio, J., Hu, S. J.,** and **Ceglarek, D.** Modeling variation propagation of multi-station assembly systems with compliant parts. *Trans. ASME, J. Mech. Des.*, 2003, **125**(4), 673–681.

30 **Camelio, J., Hu, S. J.,** and **Samuel, P. M.** Compliant assembly variation analysis using component geometric covariance. *Trans. ASME, J. Manuf. Sci. Engng*, 2004, **126**(2), 355–360.

31 **Camelio, J., Hu, S. J.,** and **Ceglarek, D.** Impact of fixture design on sheet metal assembly variation. *J. Mfg Systems*, 2004, **23**(3), 182–193.

32 **Camelio, J., Hu, S. J.,** and **Yim, H.** Sensor placement for effective diagnosis of multiple faults in fixturing of compliant parts. *Trans. ASME, J. Manuf. Sci. Engng*, 2005, **127**(1), 68–74.

33 **Rong, Q., Ceglarek, D.,** and **Shi, J.** Dimensional fault diagnosis for compliant beam structure assemblies. *Trans. ASME, J. Manuf. Sci. Engng*, 2000, **122**(4), 773–780.

34 **Rong, Q., Shi, J.,** and **Ceglarek, D.** Adjusted least squares approach for diagnosis of compliant assemblies in the presence of ill-conditioned problems. *Trans. ASME, J. Manuf. Sci. Engng*, 2001, **123**(3), 453–461.

35 **Peres, L. F.** and **DaCamara, C. C.** Inverse problems theory and application: analysis of the two-temperature method for land-surface temperature and emissivity estimation. *IEEE Trans., Geoscience and Remote Sensing Lett.*, 2004, **1**(3), 206–210.

36 **Ding, Y., Ceglarek, D.,** and **Shi, J.** Fault diagnosis of multistage manufacturing assembly processes by using state space approach. *Trans. ASME, J. Manuf. Sci. Engng*, 2002, **124**(2), 313–322.

37 **Wang, Y.** and **Nagarkar, S. R.** Locator and sensor placement for automated coordinate checking fixtures. *Trans. ASME, J. Manuf. Sci. Engng*, 1999, **121**(4), 709–719.

38 **Khan, A.** and **Ceglarek, D.** Optimization for fault diagnosis in multi-fixture assembly systems with distributed sensing. *Trans. ASME, J. Manuf. Sci. Engng*, 2000, **122**(1), 215–226.

39 **Khan, A., Ceglarek, D., Shi, J., Ni, J.,** and **Woo, T. C.** Sensor optimization for fault diagnosis in single fixture systems: a methodology. *Trans. ASME, J. Manuf. Sci. Engng*, 1999, **121**(1), 109–117.

40 **Ding, Y., Shi, J.,** and **Ceglarek, D.** Diagnosability analysis of multi-station manufacturing processes. *Trans. ASME, J. Dynamic System, Measmt, and Control*, 2002, **124**(1), 1–13.

41 **Mandroli, S. S., Shrivastava, A. K.,** and **Ding, Y.** A survey of inspection strategy and sensor distribution studies in discrete-part manufacturing processes. *IIE Trans.*, 2006, **38**(4), 309–328.

42 **Silvey, S. D.** Multicollinearity and imprecise estimation. *Technometrics*, 1969, **3**, 539–552.

43 **Golub, G. H.** and **Van Loan, C. F.** *Matrix computations*, 1983 (The Johns Hopkins University Press, Baltimore, Maryland).

44 **Van Huffel, S.** and **Vandewalle, J.** Subset selection using the total least squares approach in collinearity problems with errors in the variables. *Linear Algebra Applic.*, 1987, **88/89**, 695–714.

45 **Ceglarek, D., Huang, W., Zhou, S., Ding, Y., Kumar, R.,** and **Zhou, Y.** Time-based competition in manufacturing: stream-of-variation analysis (SOVA) methodology – review. *Int. J. Flexible Mfg Systems*, 2004, **16**(1), 11–44.

46 **Huang, W., Lin, J., Bezdecny, M., Kong, Z.,** and **Ceglarek, D.** Stream-of-variation modeling I: a generic 3D variation model for rigid body assembly in single station assembly processes. *Trans. ASME, J. Manuf. Sci. Engng*, 2007, **129**(4), 821–831.

47 **Huang, W., Lin, J., Kong, Z.,** and **Ceglarek, D.** Stream-of-variation (SOVA) modeling II: a generic 3D variation model for rigid body assembly in multi-station assembly processes. *Trans. ASME, J. Manuf. Sci. Engng*, 2007, **129**(4), 83–842.

48 **West, H.** *Analysis of structure: an integration of classical and modern methods*, 1989 (John Wiley & Sons, Inc, New York).

49 **Myers, R.** *Classical and modern regression with applications*, 1990 (Duxbury Press, Boston, Massachusetts).

50 **Jackson, J. E.** Principal components and factor analysis: Part I – principal components. *J. Quality Technol.*, 1980, **12**, 201–213.

51 **Jackson, J. E.** Principal components and factor analysis: Part II – additional topics related to principal components. *J. Quality Technol.*, 1981, **13**, 46–58.

52 **Rencher, A. C.** *Methods of multivariate analysis*, 1995 (John Wiley & Sons, Inc, New York).